Annals of Nuclear Medicine (2020) 34:815–823
https://doi.org/10.1007/s12149-020-01506-2

ORIGINAL ARTICLE

Association of tau accumulation and atrophy in mild cognitive impairment: a longitudinal study

Gang Xu[1,2] · Shuzhan Zheng[1,2] · Zhilong Zhu[1,2] · Xiaofeng Yu[1,2] · Jian Jiang[3] · Juanjuan Jiang[1,2,5] on behalf of for the Alzheimer's Disease Neuroimaging Initiative · Zhaohu Chu[4]

Received: 9 June 2020 / Accepted: 28 July 2020 / Published online: 12 August 2020

Abstract

Objective To examine the patterns of longitudinal tau accumulation and cortical atrophy and their association in subjects with mild cognitive impairment (MCI).

Methods We collected 23 participants (60–89 years old, 11 males/12 females) with MCI from the Alzheimer's Disease Neuroimaging Initiative database. All participants underwent ^{18}F flortaucipir (FTP) positron emission tomography (PET) and structural magnetic resonance imaging (MRI) scans at the baseline and follow-up visits (12–36 months). General linear models with covariates (baseline age, sex) were used to detect brain areas of significant tau accumulation and atrophy over time. Mediation analysis was employed to explore the potential reason for sequential biomarker changes in MCI progression, adjusting for baseline age, sex, and education level.

Results Voxel-wise tau accumulation in MCI subjects was predominantly located in the inferior temporal cortex, middle temporal cortex, parietal cortex, posterior cingulate, precuneus, and temporoparietal regions ($P < 0.001$), and MRI atrophy included the inferior–middle temporal lobe, parietal lobe, and precuneus ($P < 0.001$). Longitudinal FTP accumulation was moderately associated with annualized MRI cortical atrophy ($r = 0.409$, 95% CI: 0.405–0.414, $P < 0.01$). Regional analyses indicated significant bivariate associations between annualized MRI cortical atrophy and FTP accumulation (baseline FTP cortical uptake and longitudinal FTP change). The results of the mediation analysis showed that the relationship between baseline FTP uptake and longitudinal cortical atrophy was partly mediated by the longitudinal FTP cortical change (indirect effect: 0.0107, $P = 0.04$).

Conclusions Our findings provide a preliminary description of the patterns of longitudinal FTP accumulation and annualized cortical atrophy in MCI progression, and MCI subjects with high tau binding levels show an increase risk of longitudinal tau accumulation, atrophy, and cognitive decline.

Trial registration NCT00106899. Registered 1 April 2005, https://clinicaltrials.gov/ct2/show/study/NCT00106899

Keywords Tau · Flortaucipir · Atrophy · Mild cognitive impairment · Longitudinal change

Abbreviations

AD	Alzheimer's disease
APC	Annualized percentage change
CDRSB	Clinical dementia rating sum of boxes
FTP	Flortaucipir
GM	Gray matter
PVE	Partial volume effect
MCI	Mild cognitive impairment
MMSE	Mini-Mental State Examination
WM	White matter
SUVR	Standardized uptake value ratio
ROI	Region of interest

Data used in preparation of this article were obtained from the Alzheimer's Disease Neuroimaging Initiative (ADNI) database (adni.loni.usc.edu). As such, the investigators within the ADNI contributed to the design and implementation of ADNI and/or provided data, but did not participate in analysis or writing of this report. A complete listing of ADNI investigators can be found at: http://adni.loni.usc.edu/wp-content/uploads/how_to_apply/ADNI_Acknowledgement_List.pdf.

Electronic supplementary material The online version of this article (https://doi.org/10.1007/s12149-020-01506-2) contains supplementary material, which is available to authorized users.

Extended author information available on the last page of the article

Introduction

Alzheimer's disease (AD) is a complex progressive cognitive disease leading to dementia, manifesting in functional alterations and structural atrophy throughout the brain [1]. AD is typically described in focal terms: it is characterized pathologically by extracellular accumulation of amyloid-β plaques and by intracellular accumulation of neurofibrillary tangles composed of hyperphosphorylated tau [2]. Mild cognitive impairment (MCI) due to AD is the intermediate pathological stage between healthy elders and AD, and individuals with MCI are at increased risk of progressing to AD. The proposed downstream consequence of developing pathology can be visualized and quantified in living patients with positron emission tomography (PET) with various radiotracers and structural magnetic resonance imaging (MRI) [3]. Observations of pathophysiological events in the brains of clinical MCI subjects are critically important to develop an understanding of the neurodegenerative cascade progressing to AD and the relationship among protein accumulation, cortical atrophy, and cognitive impairment. The development of neurological trajectories can help to halt the progression of pathology and delay cognitive decline.

Based on postmortem studies, the cognitive deficits correlated with tau pathology are generally stronger than those correlated with amyloid-β pathology [4–6]. Converging evidence demonstrates that the development of amyloid and tau pathology may begin independently, but that amyloid-β plaques accumulate decades before cognitive symptoms and precede and accelerate the spread of tau, which further precipitates cognitive deficits [5, 7, 8]. More recently, neuroimaging studies have suggested intimate associations between the spatial pattern of tau accumulation and neuropathological alterations (i.e., cortical atrophy and glucose hypometabolism), and those neurodegeneration patterns likely interact over time [9–12]. The spatial pattern of tau may prominently intervene in the progression of MCI and preclinical AD. Recent studies on longitudinal neurological disease suggest that tau accumulation is useful to track disease progression and that tau pathology is a major driver of subsequent severe cortical atrophy [13, 14]. There are a few studies that jointly explore longitudinal tau accumulation and other related cortical atrophy. Note that a previous study analyzed longitudinal tau accumulations and discussed the relationships of changes in tau with cortical atrophy in healthy elders and patients with AD, but it did not analyze subjects with MCI [15]. Importantly, the pathophysiological process of MCI stage is critical for guiding clinical management and prevention trials.

The identification of the association between serial tau accumulation and concurrent or subsequent cortical atrophy may address the gap in our understanding of MCI progression. In the present study, we retrospectively evaluated this association using ^{18}F flortaucipir (FTP) PET and structural MRI images in a group of subjects with MCI. This study aimed to assess the patterns of longitudinal tau change and longitudinal MRI atrophy, the spatial correlation between tau accumulation and cortical atrophy, as well as the potential reason for sequential biomarker changes in MCI progression.

Materials and methods

Participants

Data in this study were obtained from the Alzheimer's Disease Neuroimaging Initiative (ADNI) database (adni.loni.usc.edu). The ADNI is a longitudinal and cross-sectional multicenter study that provides a centralized resource for clinical, brain imaging, and fluid biomarker data. The ADNI was launched in 2003 as a public–private partnership, led by Principal Investigator Michael W. Weiner, MD. The primary goal of ADNI has been to test whether serial MRI, PET, other biological markers, and clinical and neuropsychological assessment can be combined to measure the progression of MCI and early AD.

In this study, we longitudinal analyzed 23 MCI subjects who had undergone baseline tau-PET imaging with FTP and 1.5/3 T structural MRI (sMRI), as well as follow-up FTP and sMRI imaging from January 1, 2014 to February 13, 2020 (Fig. S1). Additional inclusion criteria included age between 55 and 90 years; a follow-up assessment at least 9 months after the first visit; at least 6-grade levels of education; and no serious medical, neurological, or psychiatric conditions (Clinical Dementia Rating sum of boxes (CDRSB) score > 0.5; Mini-Mental State Examination (MMSE) score > 15). All MCI subjects were clinically diagnosed by multidisciplinary experts of the ADNI according to the National Institute of Aging and Alzheimer's Association clinical criteria (detailed description in http:/adni.loni.usc.edu/methods/). Each MCI subject underwent neuropsychological assessments at baseline and follow-up, including global cognitive (CDRSB, MMSE) and specific cognitive tasks (memory, executive ability, language, and attention). The clinical characteristics and demographics of all participants are summarized in Table 1. This study was approved by the institutional review board of the ADNI, and written informed consent was obtained from all participants.

Image acquisition

The FTP-PET and sMRI image acquisitions were co-collected at the baseline and follow-up visits, and the time

Table 1 All participant characteristics

Characteristic	Value
N	23
Age (years)	73.8 ± 8.4 [60–89]
Sex (M/F), *n*	11 (47.8%)/12 (52.2%)
Education (years)	15.7 ± 2.7 [12–20]
APOE4 alleles: $n_0/n_1/n_2/n_{missing}$	6/11/5 (1)
MMSE score at baseline	26.9 ± 2.1 [19–30]
MMSE score at follow-up	23.9 ± 2.3 [17–28][a]
CDRSB score at baseline	1.47 ± 1.02 [0.5–4.5]
CDRSB score at follow-up	3.13 ± 2.1 [1–6][a]
Baseline to follow-up time (months)	14.7 ± 5.6[12–36]

Note For continuous variables, mean ± SD, range (min–max) is indicated

[a]Paired sample *t* test, $P < 0.001$

interval of the two scans within 1 month. For flortaucipir (also known as AV1451 or T807) PET imaging, participants underwent intravenous infusion with ~ 370 MBq (10 mCi) of flortaucipir (^{18}F) followed ~ 80 min later by a continuous brain PET scan acquiring six 5-min frames. FTP-PET scans were reconstructed using parameters specific to the system used for scanning. T1-weighted sMRI images were also scanned on multiple 1.5/3T MRI scanners using scanner-specific sagittal 3D Magnetization Prepared—RApid Gradient Echo (MPRAGE) sequences. Original PET and sMRI images in ADNI underwent standardized preprocessing protocols to uniform resolution to account for differences in scanner point spread function across the multicentre instruments. More detailed descriptions of PET and sMRI image acquisitions can be obtained from the ADNI database (http://adni.loni.usc.edu/methods/documents/).

Image processing

PET and sMRI image preprocessing were performed through SPM12 (Statistical Parametric Mapping 12; Wellcome Department of Imaging Neuroscience, Institute of Neurology, London, UK). We designed a longitudinal process pipeline to discover the voxel-wise change over time in both PET and MRI images. The baseline and follow-up sMRI images were processed via SPM12 pairwise longitudinal registration across individuals [16], obtaining a within-subject midpoint average MRI image and a 3-dimensional Jacobian rate map that indicated an annualized measure of volumetric contraction or expansion as described elsewhere [14, 15]. The original Jacobian maps were reversed (i.e., multiplied by − 1), so that higher positive values represented greater annualized MRI atrophy, whereas negative values represented lower annualized MRI expansion [14]. The midpoint MRI images were then segmented into probabilistic grey matter (GM), white matter (WM), and CSF maps via SPM12. The brain tissue segments were processed for further analysis, in which the GM segment from each participant's midpoint MRI was masked to exclude basal ganglia and pons and derive a subject-specific cerebral cortical mask, and the WM segment was thresholded at 0.95 and then eroded by 1 voxel to derive a subject-specific WM mask.

The FTP-PET frames were realigned and averaged to generate a PET image. The baseline and follow-up PET images were registered into the midpoint MRI space to be aligned with the reversed Jacobian rate map. The subject-specific WM mask from the midpoint MRI was used as the reference region to normalize the baseline and follow-up FTP images, because this region provided more stable estimates of FTP change [17, 18]. Partial volume effect (PVE) correction based on Muller-Gartner's algorithm was implemented using SPM's PETPVE12 toolbox [19, 20]. The normalized FTP change image of each participant was derived by subtracting the baseline FTP image from the follow-up image for each voxel. The reversed Jacobian rate map, the baseline, and follow-up FTP images and the FTP change image were warped to Montreal Neurological Institute space using the deformation parameters derived from the midpoint MRI segment. The PET images were then smoothed with a 6-mm Gaussian kernel, and the reversed Jacobian rate maps used an 8-mm Gaussian kernel. Individual annualized percentage change (APC) images of FTP change were also calculated for each voxel.

For template-warped FTP standardized uptake value ratio (SUVR) images, flortaucipir retention in the region of interest (ROI) was a surrogate for the SUVR value of each participant. The reversed Jacobian rate, SUVR values of FTP change, and APC values were calculated in 5 priori ROIs, including the inferior temporal cortex, precuneus, olfactory cortex, inferior frontal gyrus, and cerebral cortex [13, 15]. The baseline FTP SUVR value was also calculated to investigate its association with MCI progression.

Statistical analyses

Demographic and clinical characteristics at baseline were summarized with descriptive statistics across all participants (mean and standard deviation, for continuous variables; frequency and percentages for categorical information). For FTP change images, a general linear model (GLM) with covariates (baseline age, sex) was used to detect brain areas with significant tau accumulation over time (i.e., SPM's one-sample *t* test). The average APC was calculated for tau significantly changed voxels. Similarly, the reversed Jacobian rate maps also underwent a voxel-wise one-sample *t* test via GLM to reveal regions of significant atrophy over time (− Jacobians > 0). The FTP change images and reversed Jacobian rate maps were used to assess spatial correlations

between FTP accumulation and annualized MRI atrophy via Pearson correlation. All *t* test results were presented using an uncorrected voxel threshold of $P < 0.001$ (one-sided).

The baseline SUVR values, FTP change values, and reversed Jacobian rate values of the targeted ROI were entered Pearson correlation models to measure the associations between paired variables. To further explore the potential reason for sequential biomarker changes in MCI progression, all possible indirect pathways among baseline FTP, FTP change, and annualized MRI atrophy were tested via mediation analyses, adjusting for baseline age, sex, and education. Direct and indirect associations were tested using a 500-iteration bootstrapping procedure. The relationships between cognitive ability change and FTP change were assessed using simple correlation analyses. BrainNet Viewer was employed to show the imaging results [21]. All statistical analyses were implemented using MATLAB 2016b (MathWorks Inc.) and R version 3.61 (https://www.r-project.org/) employing the mediation package [22].

Results

Characteristics and descriptions of the participants

The clinical characteristics of the 23 MCI participants eligible for longitudinal analysis are summarized in Table 1. All participants underwent PET and MRI scans at the baseline and follow-up visits (mean time: 14.7 months; range: 12–36 months). MCI subjects were between 60 and 89 years old at the baseline visit (mean age: 73.8; 52.2% female). In this cohort, 72.7% of MCI subjects carried APOE4 alleles ($n = 22$, information for one was missing). Mean scores on the MMSE (26.7, range 19–30) and CDRSB (1.47, range 0.5–4.5) were comparable to values previously reported in MCI subjects [23].

Voxel-wise longitudinal MCI pattern

Figure 1 presents the pattern of longitudinal voxel-wise FTP change over time as a significance map based on a one-sample *t* test performed on the 23 FTP change images. FTP accumulation was predominantly located in the inferior temporal cortex, middle temporal cortex, parietal cortex, posterior cingulate, precuneus, and temporoparietal regions ($P < 0.001$, voxel cluster > 100). No significant FTP decrease was detected in other regions. Through FTP, significant increase masks overlaid the average APC image, and this analysis showed significant FTP annualized accumulations of 6–11% in MCI subjects.

To investigate the pattern of MRI atrophy over time in MCI subjects, we performed a longitudinal voxel-based morphometry (VBM) analysis using reversed Jacobian rate images. As shown in Fig. 2b, MRI atrophy predominantly involved the inferior–middle temporal cortex, parietal lobe, frontotemporal cortex, precuneus, and parahippocampal gyrus (one-sample *t* test; $P < 0.001$, voxel cluster > 100). There was partial overlap between the regions with significant MRI and the regions of significant FTP accumulations (Fig. 2a, b). To explore whether FTP change was independently or synergistically associated with annualized MRI atrophy, a linear model measured the correlation strength using voxel-wise statistical maps for FTP change and annualized MRI atrophy (*t*-statistic, *T* values). Longitudinal FTP accumulation was moderately associated with annualized

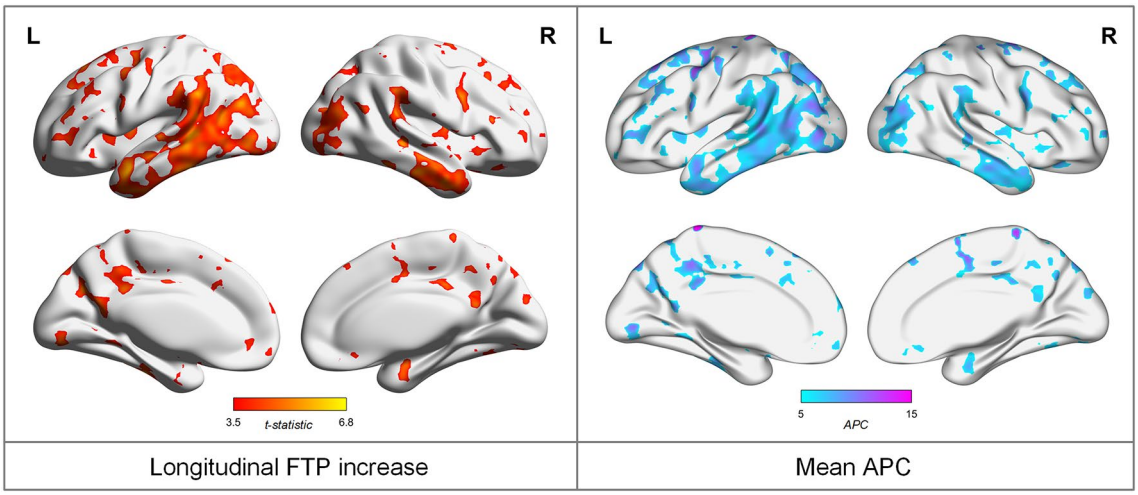

Fig. 1 The longitudinal FTP increase in MCI patients. The left panel was the result's region of one-sample *t* test where MCI patients showed a significant FTP increase over time (voxel $P < 0.001$, uncorrected). The right panel showed that voxel-wise average annualized percentage change (APC) in significant FTP change region

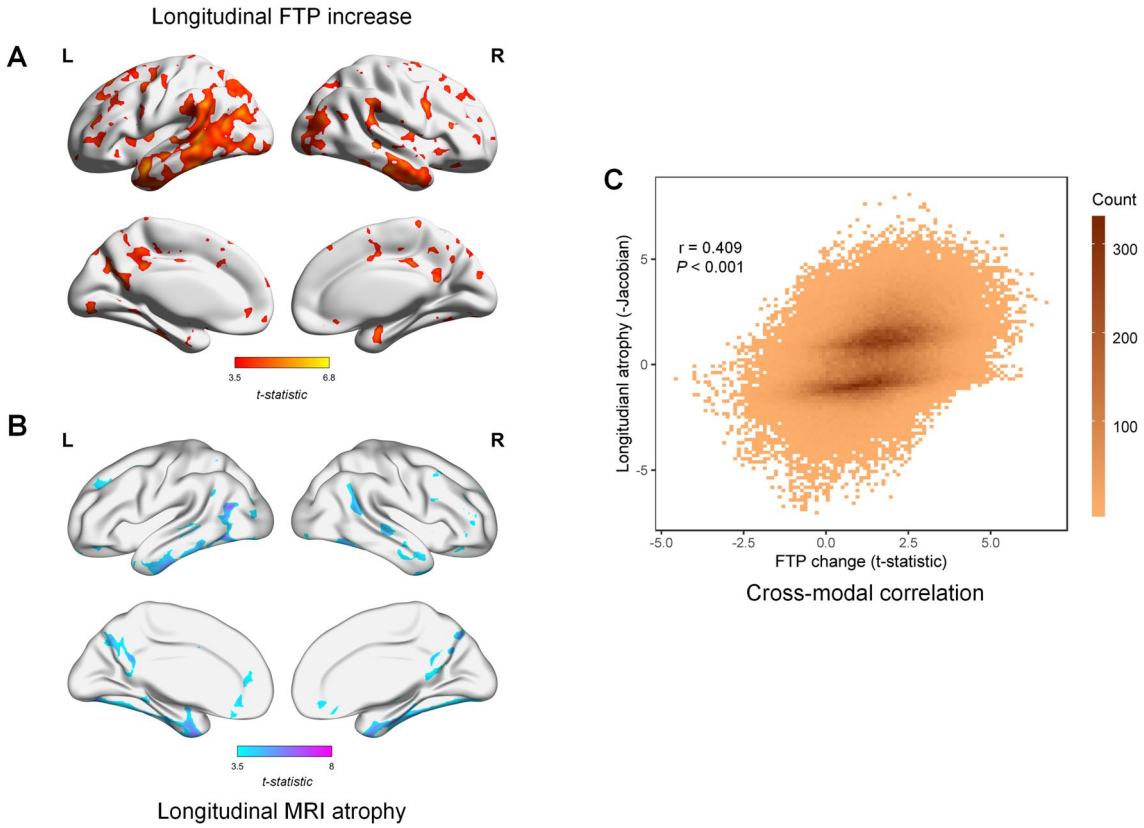

Fig. 2 The spatial statistic maps of FTP accumulation and MRI atrophy and cross-modal correlation. **a** The significant FTP change statistic map derived from FTP change images of each MCI patient ($n=23$, one-sample t test, $P<0.001$). **b** The significant MRI atrophy statistic map derived from reversed Jacobian rate map of each patient ($n=23$, one-sample t test, $P<0.001$). **c** The cross-modal correlation between FTP accumulation and MRI atrophy derived from voxel-wise statistic maps (T value). Correlation was assessed on all voxels of the cerebral cortex

MRI cortical atrophy ($r=0.409$, 95% confidence interval (CI): 0.405–0.414, $P<0.01$). These findings revealed that FTP accumulation and atrophy synergistically emerged in the progression of MCI subjects.

ROI analysis

We used regional SUVR as the surrogate to investigate the baseline FTP accumulations, longitudinal FTP change, and annualized atrophy in MCI progression. Table 2 shows that the inferior temporal cortex had a high baseline FTP uptake (mean: 1.19) in MCI subjects. MCI subjects showed

Table 2 Regional longitudinal FTP change and MRI atrophy in MCI subjects

Region	Baseline FTP SUVR	FTP change		MRI atrophy	
		APC	*P* value	− Jacobian	*P* value
ITC	1.19 ± 0.28	8.54 ± 3.16	< 0.001[a]	0.019 ± 0.003	< 0.001[a]
PCUN	1.01 ± 0.20	9.65 ± 4.49	< 0.001[a]	0.015 ± 0.004	0.003[a]
OLF	0.97 ± 0.09	6.87 ± 3.08	< 0.001[a]	0.018 ± 0.007	0.017[a]
IFG	0.99 ± 0.17	7.25 ± 2.91	< 0.001[a]	0.014 ± 0.003	< 0.001[a]
CC	1.07 ± 0.13	5.77 ± 3.49	< 0.001[a]	0.005 ± 0.001	< 0.001[a]

Note Mean ± standard deviation is given

APC annualized percentage change (%), *ITC* inferior temporal cortex, *PCUN* precuneus, *OLF* olfactory cortex, *IFG* inferior frontal gyrus, *CC* cerebral cortex

[a]Probability values indicating significant difference at $P<0.05$ (1-sided one-sample t test)

significant FTP annualized changes across all prior brain regions (all $P < 0.001$). In addition, the precuneus had the highest annualized difference (APC, 9.65% per year, $P < 0.001$) rather than other regions, and the result of annualized MRI atrophy was similar (0.015 per year, $P < 0.001$) when reversed Jacobian rate as the change parameter.

The results from voxel-wise analysis indicated that annualized MRI cortical atrophy was associated with FTP accumulation in MCI progression. We next explored the relationships between baseline FTP and subsequent longitudinal alterations (FTP change and annualized MRI atrophy) across subjects, using cerebral cortex measurements. Figure 3 shows the bivariate association between MRI cortical atrophy (mean reversed Jacobian rate in cerebral cortex) and FTP accumulation (baseline FTP cortical SUVR and longitudinal FTP change (SUVR/time)). There was a strong correlation between baseline FTP and subsequent annualized FTP increase ($r = 0.71$, 95% CI 0.43–0.78, $P < 0.001$), compared with moderate correlations with annualized MRI atrophy ($r = 0.41$, 95% CI 0.10–0.61, $P < 0.001$). Longitudinal FTP change was significantly associated with annualized MRI atrophy ($r = 0.54$, 95% CI 0.16–0.78, $P < 0.001$).

The above analysis highlighted that FTP annualized change was the strongest factor associated with baseline FTP uptake, potentially because higher baseline FTP uptake was closer to predict severe FTP change. We further explored whether the longitudinal FTP change could account for the association between baseline FTP cortical uptake and subsequent MRI atrophy. To this end, we modeled a serial mediation assessing different pathways among baseline FTP uptake, longitudinal FTP change, and annualized atrophy. We observed from Fig. 4 that the relationship between baseline FTP uptake and longitudinal atrophy was at least partly mediated by the longitudinal FTP cortical change (indirect effect: 0.0107, $P = 0.04$). After mediation, the direct association of baseline FTP uptake with MRI atrophy became nonsignificant ($P = 0.92$).

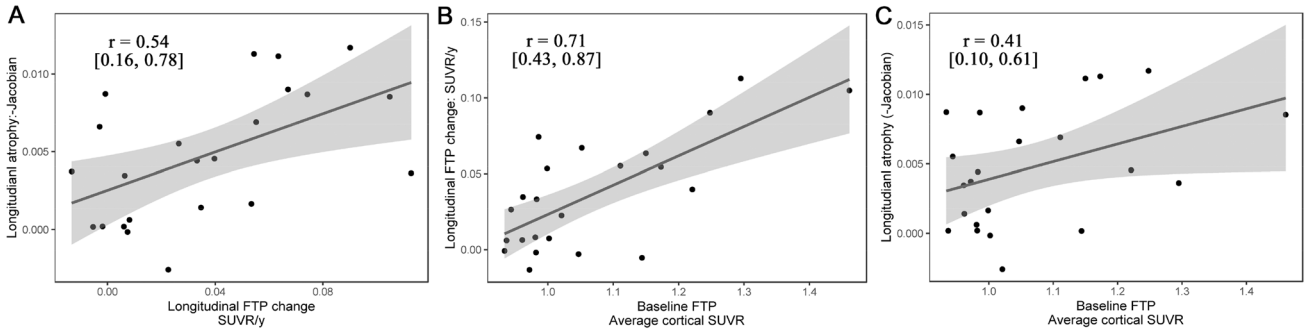

Fig. 3 Bivariate associations between baseline FTP and subsequent longitudinal FTP change/MRI atrophy across the 23 MCI patients. For 95% confidence interval (95% CI), the bootstrapping with 1000 permutations was performed

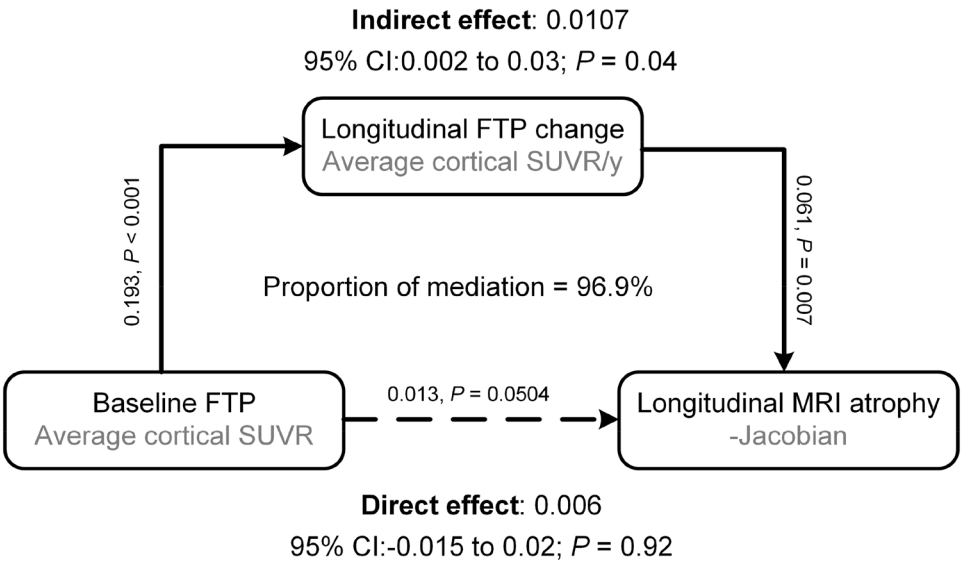

Fig. 4 Diagram of mediation model pathway relating baseline FTP, longitudinal FTP change, and MRI atrophy. Altogether, the pathways explain 96.9% of the direct effect. Mediation analysis showed that longitudinal FTP change mediated the effect of baseline FTP on longitudinal MRI atrophy

Relationship with cognitive change

MMSE and CDRSB assessments were employed to measure clinical cognitive decline. The change in these scores was annualized by (follow-up score − baseline score)/follow-up time. This analysis indicated that MMSE score changed by -2.9 ± -1.2 points per year (one-sample t test, $P < 0.001$) and CDRSB score increased by 1.25 ± 1.02 scores per year (one-sample t test, $P < 0.001$). The annualized MMSE score decrease was moderately correlated with longitudinal FTP increase ($r = -0.34$, $P < 0.01$), but was poorly correlated with longitudinal atrophy ($r = 0.12$, $P = 0.57$) and baseline FTP cortical uptake ($r = 0.13$, $P = 0.55$). There were no significant correlations between annualized CDRSB score increase and baseline FTP, longitudinal FTP change, and annualized atrophy in the cerebral cortex.

Discussion

In this longitudinal study of tau change and MRI atrophy, we examined the associations between baseline FTP binding level and subsequent neurodegeneration (FTP accumulation and annualized MRI cortical atrophy) over time across MCI subjects. In MCI progression, we observed an intimate association between FTP accumulation and cortical brain atrophy in the voxel-wise analyses, especially in the bilateral temporoparietal regions. Longitudinal FTP change has mediated the relationship between baseline FTP uptake and subsequent atrophy across MCI participants. Finally, we found that longitudinal FTP change, but not baseline FTP uptake or longitudinal cortical atrophy, was significantly correlated with the annualized cognitive change as assessed by the MMSE.

Previous neuroimaging studies examined the association between longitudinal tau change and cortical atrophy in healthy elders and AD patients, and it remained unclear what happened and which association occurred in symptomatic subjects with MCI [15]. Our study extended this gap and the main finding was the spatial topology of FTP accumulation and its annualized change rate (6–11% per year) in MCI subjects, predominantly in the middle–inferior temporal cortex. This is in line with the previous neuroimaging and pathology studies in MCI neurodegeneration showing a similar topology and spread of tau pathology [24, 25]. It is worth noting that the annualized FTP percentage change for MCI group in this work was higher than that reported for healthy elders (2–3% per year) [15]. Considering that the sensitivity of FTP and the spread pattern of FTP accumulation may be different in various clinical stages (i.e., stable MCI, developing MCI, or reversed MCI) [26, 27], the generalizability of our observed rates of longitudinal FTP accumulation in the MCI group remained to be confirmed. We further used complementary voxel-wise and ROI-based analyses to reveal the association between longitudinal FTP change and atrophy. The annualized rates of FTP accumulation and cortical atrophy were considerably stronger and were present across all prior regions. There was a moderate association between the two spatial patterns (Figs. 2 and 3). Emerging evidence suggests that tau pathology may be present before neurodegeneration starts and may propagate its effects on cognitive ability through structural pathology [28, 29]. Thus, it might be expected that the retention of tau may increase the risk of brain atrophy, in that higher tau accumulation rates and magnitudes are related to the severity of atrophy in downstream regions. This is consistent with the previous cross-sectional finding that the rate of tau accumulation correlated with the atrophy pattern over time [6, 12].

Evidence from mediation models has emerged as a plausible hypothesis that baseline cortical FTP uptake has a delayed and indirect, longitudinal FTP change-mediated association with longitudinal cortical atrophy. Previous longitudinal MRI data estimated that baseline tau pathology, rather than amyloid pathology, was a major driver of local neurodegeneration and highlighted the relevance of baseline tau uptake level as a precise way to predict individual patient cortical atrophy [14]. We observed that baseline tau uptake was closely correlated with longitudinal tau change, beyond longitudinal cortical atrophy. We also found that those individuals with high rates of tau change had elevated baseline tau uptake and atrophy, compared with individuals with low rates of tau change. These observations expand on the previous findings from longitudinal studies by providing evidence that baseline tau levels have an important role not only in longitudinal brain atrophy but also in longitudinal tau accumulation. The previous clinicopathological studies with both PET and cerebrospinal fluid data suggested that the synergy of tau and atrophy were correlated with brain dysfunction and cognitive deficits [14, 30, 31]. Together, growing evidence suggests that baseline tau uptake may reflect the presence of subsequent tau change, which has the ability to predict cortical atrophy over time. These findings had potential ramifications for clinical trials in that tau-based measurements might be superior for tracking pathology trajectories during MCI progression. Contrary to expectations, we observed that clinical cognitive change as assessed by MMSE score was associated only with longitudinal cortical FTP increase. There were no significant correlations between clinical decline and baseline tau uptake, or longitudinal cortical atrophy. These weak correlations may be related to the small sample size or intrinsic noise interferences in both clinical assessments and imaging [14].

A strength of this retrospective study was that we used longitudinal FTP-PET and structural MRI imaging in individuals across the MCI spectrum. There are some limitations that should be noted to appropriately interpret our results.

First, the small sample size may have limited our statistical power and prevented generalization, and especially to explore the patterns of longitudinal tau change and annualized cortical atrophy (uncorrected *P* value). Second, the MCI subjects of this study were collected from the ADNI database, which may limit the number of follow-up visits (only two-time points) and additional follow-up visits would enable a more detailed characterization of neurodegeneration trajectories. Third, our cohort included only subjects in the MCI stage, and therefore, the data could not be extrapolated to subjects with AD continuum, and future work will be needed to determine the straightforward pathological association over the total AD continuum; Finally, our MCI cohort lacked unabridged amyloid PET data to determine the amyloid status. The association between cortical atrophy and cognitive may be different in opposite amyloid status. The coexistence of amyloid and tau-PET images may help to determine more comprehensive pathological trajectories.

Conclusions

In summary, in this longitudinal study, we investigated the voxel-wise patterns of tau accumulation and cortical atrophy over time and neurodegeneration trajectories in symptomatic subjects with MCI. These results suggested that baseline cortical FTP uptake had a delayed and indirect, longitudinal FTP change-mediated association with longitudinal cortical atrophy. These findings highlight the importance of tau-based measurements to track MCI degeneration and further halt pathological progression and delay cognitive deficits.

Acknowledgements Data collection and sharing for this project was funded by the Alzheimer's Disease Neuroimaging Initiative (ADNI) (National Institutes of Health Grant U01 AG024904) and DOD ADNI (Department of Defense award number W81XWH-12-2-0012). ADNI is funded by the National Institute on Aging, the National Institute of Biomedical Imaging and Bioengineering, and through generous contributions from the following: AbbVie, Alzheimer's Association; Alzheimer's Drug Discovery Foundation; Araclon Biotech; BioClinica, Inc.; Biogen; Bristol-Myers Squibb Company; CereSpir, Inc.; Cogstate; Eisai Inc.; Elan Pharmaceuticals, Inc.; Eli Lilly and Company; EuroImmun; F. Hoffmann-La Roche Ltd and its affiliated company Genentech, Inc.; Fujirebio; GE Healthcare; IXICO Ltd.; Janssen Alzheimer Immunotherapy Research & Development, LLC.; Johnson & Johnson Pharmaceutical Research & Development LLC.; Lumosity; Lundbeck; Merck & Co., Inc.; Meso Scale Diagnostics, LLC.; NeuroRx Research; Neurotrack Technologies; Novartis Pharmaceuticals Corporation; Pfizer Inc.; Piramal Imaging; Servier; Takeda Pharmaceutical Company; and Transition Therapeutics. The Canadian Institutes of Health Research is providing funds to support ADNI clinical sites in Canada. Private sector contributions are facilitated by the Foundation for the National Institutes of Health (www.fnih.org). The grantee organization is the Northern California Institute for Research and Education, and the study is coordinated by the Alzheimer's Therapeutic Research Institute at the University of Southern California. ADNI data are disseminated by the Laboratory for Neuro Imaging at the University of Southern California.

Author contributions GX designed the study. GX and SZZ collected the data. ZLZ and XFY developed the experimental model and analyzed the data. JJJ performed the clinical assessments and supported the analysis. JJ provided guidance for medical statistics in this study. ZHC, JJJ, and GX supervised the study. All authors interpreted the data results, drafted, and edited the manuscript.

Funding This work was supported by grants from the Key Project of Natural Science in Universities in Anhui Province (KJ2018A0111), Open Research Fund of Anhui Key Laboratory of Detection Technology and Energy Saving Devices, Anhui Polytechnic University (2017070503B026-A01).

Availability of data and materials Please contact the corresponding author for data requests or download from the ADNI database (http://adni.loni.usc.edu/).

Compliance with ethical standards

Conflict of interest The authors declare that they have no competing interests.

Ethics approval All procedures performed in studies involving human participants were in accordance with the ethical standards of the institutional and/or national research committee and with the 1964 Helsinki Declaration and its later amendments or comparable ethical standards. All MCI subjects signed written consent for the evaluation of their data and the institutional review board of the ADNI approved this analysis.

References

1. Alzheimer's Association. 2019 Alzheimer's disease facts and figures. Alzheimer's Dementia. 2019;15(3):321–87.
2. Hyman BT, Phelps CH, Beach TG, Bigio EH, Cairns NJ, Carrillo MC, et al. National Institute on Aging-Alzheimer's Association guidelines for the neuropathologic assessment of Alzheimer's disease. Alzheimer's Dementia: J Alzheimer's Assoc. 2012;8(1):1–13.
3. Jagust W. Imaging the evolution and pathophysiology of Alzheimer disease. Nat Rev Neurosci. 2018;19(11):687–700.
4. Giannakopoulos P, Herrmann FR, Bussiere T, Bouras C, Kovari E, Perl DP, et al. Tangle and neuron numbers, but not amyloid load, predict cognitive status in Alzheimer's disease. Neurology. 2003;60(9):1495–500.
5. Nelson PT, Alafuzoff I, Bigio EH, Bouras C, Braak H, Cairns NJ, et al. Correlation of Alzheimer disease neuropathologic changes with cognitive status: a review of the literature. J Neuropathol Exp Neurol. 2012;71(5):362–81.
6. Bejanin A, Schonhaut DR, La Joie R, Kramer JH, Baker SL, Sosa N, et al. Tau pathology and neurodegeneration contribute to cognitive impairment in Alzheimer's disease. Brain. 2017;140(12):3286–300.
7. Jack CR Jr, Knopman DS, Jagust WJ, Petersen RC, Weiner MW, Aisen PS, et al. Tracking pathophysiological processes in Alzheimer's disease: an updated hypothetical model of dynamic biomarkers. Lancet Neurol. 2013;12(2):207–16.
8. Nelson PT, Jicha GA, Schmitt FA, Liu H, Davis DG, Mendiondo MS, et al. Clinicopathologic correlations in a large Alzheimer disease center autopsy cohort: neuritic plaques and neurofibrillary tangles "do count" when staging disease severity. J Neuropathol Exp Neurol. 2007;66(12):1136–46.

9. Cho H, Choi JY, Hwang MS, Lee JH, Kim YJ, Lee HM, et al. Tau PET in Alzheimer disease and mild cognitive impairment. Neurology. 2016;87(4):375–83.
10. Nasrallah IM, Chen YJ, Hsieh MK, Phillips JS, Ternes K, Stockbower GE, et al. (18)F-Flortaucipir PET/MRI correlations in nonamnestic and amnestic variants of Alzheimer disease. J Nucl Med Off Publ Soc Nucl Med. 2018;59(2):299–306.
11. Jack CR Jr, Wiste HJ, Weigand SD, Therneau TM, Lowe VJ, Knopman DS, et al. Defining imaging biomarker cut points for brain aging and Alzheimer's disease. Alzheimer's Dementia: J Alzheimer's Assoc. 2017;13(3):205–16.
12. Xia C, Makaretz SJ, Caso C, McGinnis S, Gomperts SN, Sepulcre J, et al. Association of in vivo [18F]AV-1451 tau PET imaging results with cortical atrophy and symptoms in typical and atypical Alzheimer disease. JAMA Neurol. 2017;74(4):427–36.
13. Hanseeuw BJ, Betensky RA, Jacobs HIL, Schultz AP, Sepulcre J, Becker JA, et al. Association of amyloid and tau with cognition in preclinical Alzheimer disease: a longitudinal study. JAMA Neurol. 2019;76(8):915–24. https://doi.org/10.1001/jamaneurol.2019.1424.
14. La Joie R, Visani AV, Baker SL, Brown JA, Bourakova V, Cha J, et al. Prospective longitudinal atrophy in Alzheimer's disease correlates with the intensity and topography of baseline tau-PET. Sci Transl Med. 2020;12(524):eaau5732. https://doi.org/10.1126/scitranslmed.aau5732.
15. Harrison TM, La Joie R, Maass A, Baker SL, Swinnerton K, Fenton L, et al. Longitudinal tau accumulation and atrophy in aging and alzheimer disease. Ann Neurol. 2019;85(2):229–40.
16. Ashburner J, Ridgway GR. Symmetric diffeomorphic modeling of longitudinal structural MRI. Front Neurosci. 2012;6:197.
17. Fleisher AS, Joshi AD, Sundell KL, Chen YF, Kollack-Walker S, Lu M, et al. Use of white matter reference regions for detection of change in florbetapir positron emission tomography from completed phase 3 solanezumab trials. Alzheimer's Dementia: J Alzheimer's Assoc. 2017;13(10):1117–24.
18. Southekal S, Devous MD Sr, Kennedy I, Navitsky M, Lu M, Joshi AD, et al. Flortaucipir F 18 quantitation using parametric estimation of reference signal intensity. J Nucl Med: Off Publ Soc Nucl Med. 2018;59(6):944–51.
19. Muller-Gartner HW, Links JM, Prince JL, Bryan RN, McVeigh E, Leal JP, et al. Measurement of radiotracer concentration in brain gray matter using positron emission tomography: MRI-based correction for partial volume effects. J Cereb Blood Flow Metab. 1992;12(4):571–83.
20. Gonzalez-Escamilla G, Lange C, Teipel S, Buchert R, Grothe MJ. Alzheimer's disease neuroimaging I. PETPVE12: an SPM toolbox for partial volume effects correction in brain PET—application to amyloid imaging with AV45-PET. Neuroimage. 2017;147:669–77.
21. Xia M, Wang J, He Y. BrainNet Viewer: a network visualization tool for human brain connectomics. PLoS ONE. 2013;8(7):e68910.
22. Tingley D, Yamamoto T, Hirose K, Keele L, Imai K. Mediation:RPackage for causal mediation analysis. J Stat Softw. 2014;59(5):38.
23. Jansen WJ, Ossenkoppele R, Knol DL, Tijms BM, Scheltens P, Verhey FR, et al. Prevalence of cerebral amyloid pathology in persons without dementia: a meta-analysis. JAMA. 2015;313(19):1924–38.
24. Hanseeuw BJ, Betensky RA, Schultz AP, Papp KV, Mormino EC, Sepulcre J, et al. Fluorodeoxyglucose metabolism associated with tau-amyloid interaction predicts memory decline. Ann Neurol. 2017;81(4):583–96.
25. Adams JN, Lockhart SN, Li L, Jagust WJ. Relationships between tau and glucose metabolism reflect Alzheimer's disease pathology in cognitively normal older adults. Cereb Cortex. 2019;29(5):1997–2009.
26. Josephs KA, Whitwell JL, Tacik P, Duffy JR, Senjem ML, Tosakulwong N, et al. [18F]AV-1451 tau-PET uptake does correlate with quantitatively measured 4R-tau burden in autopsy-confirmed corticobasal degeneration. Acta Neuropathol. 2016;132(6):931–3.
27. Smith R, Puschmann A, Scholl M, Ohlsson T, van Swieten J, Honer M, et al. 18F-AV-1451 tau PET imaging correlates strongly with tau neuropathology in MAPT mutation carriers. Brain. 2016;139(Pt 9):2372–9.
28. Spillantini MG, Goedert M. Tau protein pathology in neurodegenerative diseases. Trends Neurosci. 1998;21(10):428–33.
29. Jack CR Jr, Holtzman DM. Biomarker modeling of Alzheimer's disease. Neuron. 2013;80(6):1347–58.
30. Wang L, Benzinger TL, Su Y, Christensen J, Friedrichsen K, Aldea P, et al. Evaluation of tau imaging in staging Alzheimer disease and revealing interactions between β-amyloid and tauopathy. JAMA Neurol. 2016;73(9):1070–7.
31. Sepulcre J, Grothe MJ, Sabuncu M, Chhatwal J, Schultz AP, Hanseeuw B, et al. Hierarchical organization of tau and amyloid deposits in the cerebral cortex. JAMA Neurol. 2017;74(7):813–20.

Affiliations

Gang Xu[1,2] · Shuzhan Zheng[1,2] · Zhilong Zhu[1,2] · Xiaofeng Yu[1,2] · Jian Jiang[3] · Juanjuan Jiang[1,2,5] on behalf of for the Alzheimer's Disease Neuroimaging Initiative · Zhaohu Chu[4]

✉ Juanjuan Jiang
jiangjuanjuan@ahpu.edu.cn

✉ Zhaohu Chu
chuzhaohu878@163.com

[1] Key Laboratory of Advanced Perception and Intelligent Control of High-end Equipment, Ministry of Education, Wuhu 241000, China

[2] School of Electrical Engineering, Anhui Polytechnic University, Wuhu 241000, China

[3] Center of Reproductive Medicine, Yijishan Hospital of Wannan Medical College, Wuhu 241001, Anhui, China

[4] Department of Neurology, Yijishan Hospital of Wannan Medical College, Wuhu 241000, Anhui, China

[5] Key Laboratory of Advanced Perception and Intelligent Control of High-End Equipment, Ministry of Education, Anhui Polytechnic University, 8 Beijing Middle Road, Wuhu 241000, People's Republic of China